THE JOURNAL OF PHYSICAL CHEMISTRY B
A JOURNAL OF THE AMERICAN CHEMICAL SOCIETY

pubs.acs.org/JPCB

Article

Understanding X-ray Photoelectron Spectra of Ionic Liquids: Experiments and Simulations of 1-Butyl-3-methylimidazolium Thiocyanate

Published as part of The Journal of Physical Chemistry virtual special issue "Early-Career and Emerging Researchers in Physical Chemistry Volume 2".

Ekaterina Gousseva, Scott D. Midgley, Jake M. Seymour, Robert Seidel, Ricardo Grau-Crespo, and Kevin R. J. Lovelock*

Cite This: *J. Phys. Chem. B* 2022, 126, 10500−10509

Read Online

ACCESS | Metrics & More | Article Recommendations | Supporting Information

ABSTRACT: We demonstrate a combined experimental and computational approach to probe the electronic structure and atomic environment of an ionic liquid, based on core level binding energies. The 1-butyl-3-methylimidazolium thiocyanate $[C_4C_1Im][SCN]$ ionic liquid was studied using ab initio molecular dynamics, and results were compared against previously published and new experimental X-ray photoelectron spectroscopy (XPS) data. The long-held assumption that initial-state effects in XPS dominate the measured binding energies is proven correct, which validates the established premise that the ground state electronic structure of the ionic liquid can be inferred directly from XPS measurements. A regression model based upon site electrostatic potentials and intramolecular bond lengths is shown to account accurately for variations in core-level binding energies within the ionic liquid, demonstrating the important effect of long-range interactions on the core levels and throwing into question the validity of traditional single ion pair ionic liquid calculations for interpreting XPS data.

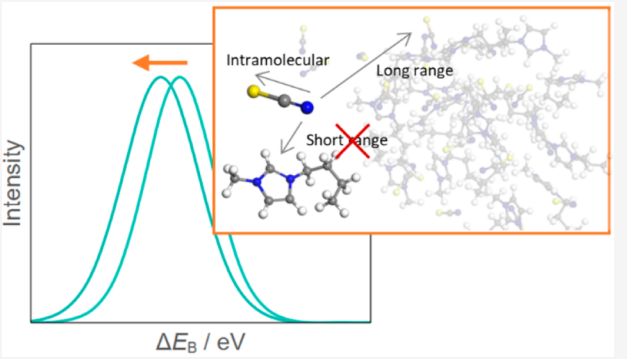

1. INTRODUCTION

Ionic liquids (ILs) are liquids composed exclusively of ions. Their interesting potential properties, including large electrochemical windows, wide liquid ranges, tunability, and low melting points,[1,2] make then desirable for a range of applications, from catalysis to batteries.[3−7] Macro- and mesoscopic properties, unique to each IL, are determined by interactions between the cation and anions.[8] A thorough study of molecular-level interactions in ILs could lead to a method to predict structure, properties, and reactivity[9,10] and eventually suitability for specific applications. The donation of electron density from anion to cation, often termed charge transfer, has been debated in the IL literature, along with the importance of ion polarizability.[11,12] The distance dependence of electronic cation−anion interion interactions for ILs, particularly important for understanding the dynamics of ILs, is currently unclear. Furthermore, the range of electronic environments present in the IL has been probed computationally, but not compared to experimental data.[13,14]

X-ray photoelectron spectroscopy (XPS) is a very useful tool to understand these interactions. XPS has traditionally been used on solid or gaseous samples, due to the required ultrahigh-vacuum conditions (UHV).[15,16] XPS can, however, be applied to ILs as they exhibit very low vapor pressure and therefore are part of a limited group of liquids that can be studied using standard UHV XPS apparatus.[17−19] XPS has been used for ILs to probe both surface geometric structure (e.g., by varying the IL surface detector angle)[20−22] and bulk electronic structure.[1] The study of ILs via XPS offers many opportunities, but also faces several obstacles.

Core-level binding energies, E_B, can be used to understand the electronic structure of ILs as E_B is the difference between the ground state and an excited state with a core hole.[23,24] E_B shifts are caused by valence electron behavior, which in turn is affected by the chemical environment around the ion. The position of the core level in the ground state, relative to the vacuum (or at times the Fermi level for experimental data), determines what is called the initial-state (IS) effect in E_B. The

Received: September 6, 2022
Revised: November 4, 2022
Published: December 1, 2022

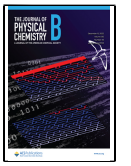

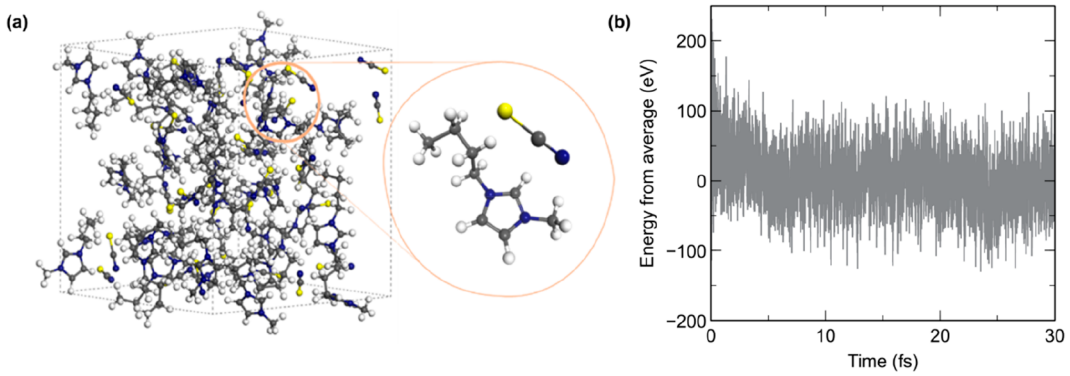

Figure 1. (a) Simulation cell used in this work, which is repeated under periodic boundary conditions. The cell consists of 32 pairs of $[C_4C_1Im][SCN]$ to create a disordered liquid phase. (b) Potential energy of the system at each time step over the course of the AIMD calculation. A configuration for further core-hole calculations was taken at a step with average energy to produce 32 conformers.

ground-state electronic structure is related to the atomic environment, i.e., bonding and interactions. When an electron is photoemitted from the core level, the other core and valence electrons relax. The magnitude of this relaxation affects the E_B value and is called the final-state (FS) effect.

Interion electronic effects of the anion on the cation have been demonstrated using XPS; however, whether this effect is due principally to IS or FS effects is unclear.[25] It is usually assumed for XPS of ILs that IS effects dominate the measured E_B.[25−65] It is an important assumption because, if correct, it means that experimental E_B shifts give valuable clues about the ground-state electronic structure of ILs. Many studies have been performed under this assumption, relating E_B of core levels to atomic charge, oxidation state, or electronegativity, to understand and potentially make predictions on structure and reactivity.[25−65] However, this assumption has so far proved impossible to establish exclusively using experimental methods; core-level E_B values have been compared to shifts in near-edge X-ray absorption fine structure (NEXAFS) spectroscopy edge energies and Auger parameter values to try to determine the relative influence of IS and FS effects in XPS for ILs.[66,67]

The combination of experimental E_B and theoretical models to study ILs has had limited use to date. It has been applied to study partial charges and models of a single ion or a pair (one anion with one cation).[25,64,65,67,68] Two studies reported calculations on larger model systems (ion "clusters", up to eight ion pairs), but comparisons were only made for valence levels, not for core levels.[69,70] Comparisons of core E_B to calculated atomic charges have also been made, which are based on the assumption that IS effects dominate E_B shifts.[25,64,66,67,69] E_B of core levels have been calculated for ILs,[65] but rarely are core holes explicitly included and only on small scale systems such as lone ions or ion pairs.[38,68]

The XPS signal from an IL arises from contributions from a distribution of E_B values that reflects the range of chemical environments coexisting in the IL. Thus, the broadening of an experimental XPS core level peak has the potential to give information about the geometric structure of a sample.[71] The full width at half-maximum (FWHM) of a measured core-level peak will contain contributions from a range of factors, including X-ray source and analyzer resolution from the apparatus,[72] charging,[73] core-hole lifetime,[74] and sample geometric structure effects.[75] For XPS of liquids, only water FWHMs have been widely published; the structural disorder contribution to the FWHM for liquid phase water and ions solvated in water is around 1.0 eV.[75,76] The experimental FWHM was interpreted in relation to the liquid phase geometric structure, e.g., the hydrogen bonding in liquid water.[76] For ILs, no investigations of the structural disorder contribution to the FWHM have been made. Developments in *ab initio* molecular dynamics (AIMD) have seen improvements in speed and accuracy,[77] which has allowed its use in the simulation of ILs.[77−92] Despite this, no theoretical studies of core levels in bulk liquid phase with explicit ions have been performed on ILs, to the best of our knowledge. A combined approach is required, including computer simulations validated by experimental data, such as peak positions and broadening.

In this work, we present a theoretical study of core-level E_B values and distribution in a bulk IL system, $[C_4C_1Im][SCN]$. Experimental XPS data are available for $[C_4C_1Im][SCN]$ in the literature.[66,67] AIMD is used here to simulate a bulk model of this IL, which was chosen due to desirable properties of both the anion and the cation. $[C_4C_1Im]^+$ is one of the most commonly studied cations, and further understanding of its behaviors will be an asset in several areas of research. Its relatively small size is convenient for expensive AIMD calculations. The anion, $[SCN]^-$, is also small. The negatively charged S and N atoms potentially allow for hydrogen bonds to be created in the bulk system.[66,67] $[SCN]^-$ is particularly interesting as it is a pseudohalide, yet $[C_4C_1Im][SCN]$ has one of the lowest viscosities among ILs,[93] in contrast to $[C_4C_1Im][PF_6]$, for example.[94] Core E_B values were calculated using density functional theory according to two approximations: (i) including IS effects only (we call this the IS approximation) and (ii) including both IS and FS effects via explicit consideration of the core hole (we call this the FS approximation). We demonstrate an excellent match between experiment and calculations. We show that IS effects are the major contributor to experimental core level E_B, a significant contribution to the sphere of researching ILs using XPS methods. Variation of E_B(core) was assessed in relation to a range of interactions, which is only possible in a calculation of the bulk liquid, as opposed to considering only single ions or ion pairs. A model that describes the variations of E_B within the IL is presented. The structural disorder contribution to FWHM was compared between theory and experiment.

2. METHODS

2.1. X-ray Photoelectron Spectroscopy (XPS). Liquid jet XPS measurements for K[SCN] in water were performed at

https://doi.org/10.1021/acs.jpcb.2c06372
J. Phys. Chem. B 2022, 126, 10500−10509

the U49/2 PGM-1 beamline (SOL^{3}PES end-station) at the BESSY II electron storage ring.[95] The SOL^{3}PES experimental setup is equipped with a Scienta Omicron R4000 HIPP-2 hemispherical electron analyzer. K[SCN] (Sigma-Aldrich, purity ≥99.0%) was dissolved in ultrapure water. The mole fraction of K[SCN] in water was x = 0.01, i.e., 0.5 M. Nonresonant XPS regions were recorded at $h\nu$ = 700.0 eV. The pass energy was 100 eV. The angle between the polarization axis of the incoming photon beam and the electron analyzer was 54.7° (magic angle geometry). All nonresonant XP spectra were fitted using the CASAXPS software. Fitting was performed using a Shirley background and GL30 line shapes (70% Gaussian, 30% Lorentzian). Photoelectron spectra E_B for [C_4C_1Im][SCN] were effectively charge referenced to the literature value of $E_B(C_{alkyl}\ 1s)$ = 289.58 eV (which corresponds to alignment with vacuum).[96] Photoelectron spectra E_B for K[SCN] in water were charge referenced to $E_B(N_{anion}\ 1s)$ = 402.37 eV, as $E_B(N_{anion}\ 1s)$ = 402.37 eV for [C_4C_1Im][SCN] when charge referenced to $E_B(C_{alkyl}\ 1s)$ = 289.58 eV. Experimental data for all [C_4C_1Im][SCN] measurements were taken from an earlier publication by our group,[109] where all the experimental details may be found.

2.2. *Ab Initio* Molecular Dynamics (AIMD). A 32 ion pair model of [C_4C_1Im][SCN] with a density of 1.07 g cm^{-3} [97] was simulated using AIMD with the Quickstep code in CP2K, based on the Gaussian and plane waves method (GPW) and using the direct inversion in iterative subspace (DIIS) technique. After pre-equilibration using the classical force field DREIDING, the AIMD simulation was run for 30 ps with a time step of 1 fs. The potential energy variations were equilibrated after <10 ps of AIMD. This simulation was performed at 398 K controlled by a Nosé thermostat in the NVT ensemble. The PBE functional[98] was employed, with D2 corrections by Grimme[99,100] to account for dispersion interactions. A configuration at the end of the simulation, with energy close to the average, was extracted to carry out core-level calculations. An increased temperature of 398 K reduces viscosity and allows for equilibrium to be achieved faster, thus reducing the computational cost of the calculation while remaining in a range safe from thermal decomposition.

2.3. Core-Level Calculations in Bulk Ionic Liquid. Calculations of E_B(core) were performed in the Vienna Ab Initio Simulation Package (VASP).[101] A snapshot configuration with an energy close to the AIMD average was chosen to calculate the distribution of E_B values across the 32 ion pairs. The core-level calculations also used the PBE exchange correlation functional employed for the AIMD. The core−valence electron interactions were described using projector augmented wave (PAW) potentials.[102,103] The number of plane waves in the basis set expansion of the wave functions was chosen by setting the kinetic energy cutoff to 400 eV. All core level energies of the system were calculated in this same configuration, for IS and FS. Test calculations showed that the distribution of binding energies was not significantly affected by choosing or adding other configurations.

The IS approximation to calculating E_B(core), as defined in this work, is obtained from the Kohn−Sham (KS) orbital energies. The KS orbital energies are calculated after a self-consistent calculation of the valence charge density. No core hole is produced, and therefore any core-hole-related effects are omitted. Only IS effects influence E_B and the orbital energies, or core levels (CL), are converted to E_B simply, by

$$E_B = -CL \tag{1}$$

These values, as obtained from VASP, are aligned with an internal energy reference, so only relative values are meaningful. Here, we shifted the calculated core-level values to match experiment, as explained below.

In contrast, for the FS approximation, the calculation involves creating a core hole explicitly. In the FS method used in VASP, it is assumed the nuclei are static, due to the time scale of the excitation of an electron. Additionally, the other core electrons in the atom are not allowed to relax once the core hole has been created. This may create a slight error, specifically in relation to a lack of lifetime broadening of the resultant peak. The energy extracted is the total energy of the system, including the core hole. This means that the calculated energy is again useless as an absolute energy, and only relative energies can be used. In this work, we have aligned the average FS energy with the average IS energy, to give FS values that are comparable with experiment. This method provides an internal comparison of values; i.e., the absolute value has no inherent meanings, other than its relation to other E_B values. Absolute energies were not considered, but rather the difference between energies (ΔE_B).

2.4. Molecular Calculations. Test calculations of isolated [SCN]$^-$ anions were performed using Gaussian16.[104] These single point energy calculations were performed with the 6-31g(d, p) basis set[105,106] and the B3LYP functional.[107] These tests were designed to separate intraion from interion contributions to E_B. Intraion interactions were characterized by the lengths of S−C and N−C anion bonds. One bond was kept constant while the other was modified. The constant bond length was determined by taking an average of the 32 bond lengths in the configuration. For S−C this was 1.65 Å, and for N−C it was 1.20 Å. The same method in Gaussian16, as above, was used to optimize the ions with the second bond length varied at an interval of 0.02 Å, and the E_B was extracted from orbital energies. We studied short-range interactions by extracting radial distribution functions (RDFs) and visually assessing each anionic environment.

2.5. Gaussian−Lorentzian Peaks. A Gaussian−Lorentzian Product (GLP) function is one of several types of functions used to fit peaks in experimental XPS measurements.[108] XPS peaks are typically expected to be Lorentzian, but due to the various sources of broadening, this shape is distorted and compensated for by including Gaussian mixing in the function. To form a peak from the 32 data points for each core level, eq 2 was applied to the values, where the mixing parameter, m, was set to 0.3 as in experimental peak fitting. Values 0 and 1 are pure Gaussian and pure Lorentzian, respectively. The function width, F, was set at either 0.7 or 1 eV for high resolution and survey scan peaks, respectively.

$$\mathrm{GLP}(x; F, E, m) = \exp\left[-4\ln 2(1-m)\frac{(x-E)^2}{F^2}\right] \Big/ \left[1 + 4m\frac{(x-E)^2}{F^2}\right] \tag{2}$$

In the investigation of ILs using XPS, survey scans are typically used to determine the presence of impurities of the sample. They are measured to see what elements are present, and their abundance, using a high pass energy and low resolution. These settings result in greater apparatus broadening contributions to the peaks. High-resolution scans are measured with low pass

https://doi.org/10.1021/acs.jpcb.2c06372
J. Phys. Chem. B 2022, 126, 10500−10509

energy. These are used to identify chemical states and typically have lower broadening than survey scans. Calculated peaks were slightly shifted in position and normalized by intensity for improved comparison with experiment. Values were shifted by +21.2 and +27.0 eV and intensities corrected by the height of the C 1s peak.

3. RESULTS AND DISCUSSION

3.1. Initial-State vs Final-State Approximations to the Core-Level Binding Energies. A comparison between calculated binding energies in the IS and FS approximations was performed to identify the dominant effects. Because the calculation in the FS approximation includes both IS and FS effects, a strong positive linear correlation (Figure 2) is

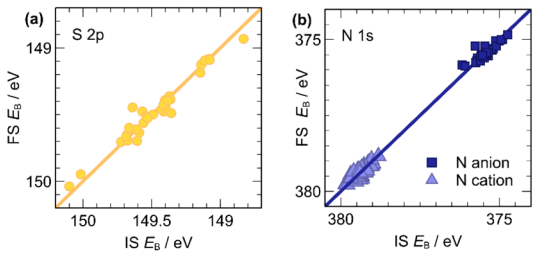

Figure 2. Linear correlations between binding energies calculated in IS and FS approximations for (a) E_B (S 2p) and (b) E_B(N 1s). The $y = x$ line is plotted as a guide. $R^2 = 0.95$ (a), 0.77 (b, anion), and 0.74 (b, cation).

reasonable confirmation that FS effects are minor, and therefore IS effects are the primary influence on E_B(core). E_B(S 2p) values calculated in the FS approximation showed strong correlations with the corresponding values calculated in the IS approximation ($R^2 = 0.950$). Correlation between results in the IS and FS approximations was also good for E_B(N 1s) ($R^2 = 0.995$), although the correlation is weaker if N_{anion} and N_{cation} are considered separately ($R^2 = 0.77$ and $R^2 = 0.74$, respectively). The reason the E_B(N 1s) were more affected by FS effects than $E_B(S_{anion}$ 2p) was investigated further, and it will be discussed below.

The deviations from the $y = x$ line in these plots are due to final-state effects. However, these deviations are small in comparison with the spread of the values: in Figure 2a (for S 2p core levels) the maximum absolute deviation is 0.19 eV, and the mean absolute deviation is only 0.04 eV, in a range of 1.3 eV. In Figure 2b (for N 1s core levels), the maximum absolute deviation is 0.54 eV, but the mean absolute deviation is only 0.09 eV, in a range of over 5 eV.

The conclusion about the absence of strong FS effects is important because it means that XPS E_B can be related directly to the ground-state electronic structure of the IL, which is the primary reason we turn to XPS to study these systems. Furthermore, it facilitates our theoretical study of the distribution of core-level binding energies in the IL bulk liquid because calculations in the IS approximation are computationally cheaper and much simpler: one single-point calculation is enough, whereas in the FS approximation, individual calculations explicitly including a core hole at each atom in the liquid are required. In what follows, the reported binding energies were obtained in the IS approximation, unless otherwise stated.

Having established the validity of the IS approximation, the accuracy of the calculated distribution of E_B(core) was tested against experiment. The experimental survey XP spectrum was plotted and compared against our calculated survey spectrum (Figure 3). Quantitative and qualitative analyses of neighboring peaks showed the overall accuracy of the computed results to be high, despite the omission of FS effects. Most E_B separations are within a 3.5% deviation from experiment. In particular, a high-resolution scan comparison shows $\Delta E_B = E_B(N_{cation}$ 1s) $- E_B(N_{anion}$ 1s) is 4.1 eV in experiment and 4.0 eV in calculated peaks (Figure 3b), which are in excellent agreement. The only significant discrepancy in the survey scan plot is a calculated 55.2 eV separation between S 2s and S 2p levels, whereas in experiment the separation was 64.2 eV; this is almost a 9 eV change between the two sets of results, or a 14% error.

A comparison of C 1s peaks further confirmed the success of the IS calculations in replicating experimental measurements. Our new experimental data have shown the position of the C 1s anion peak from $[SCN]^-$, previously unidentified, alongside a fitting model used for the C 1s peak (Figure 4a).[109] Visual

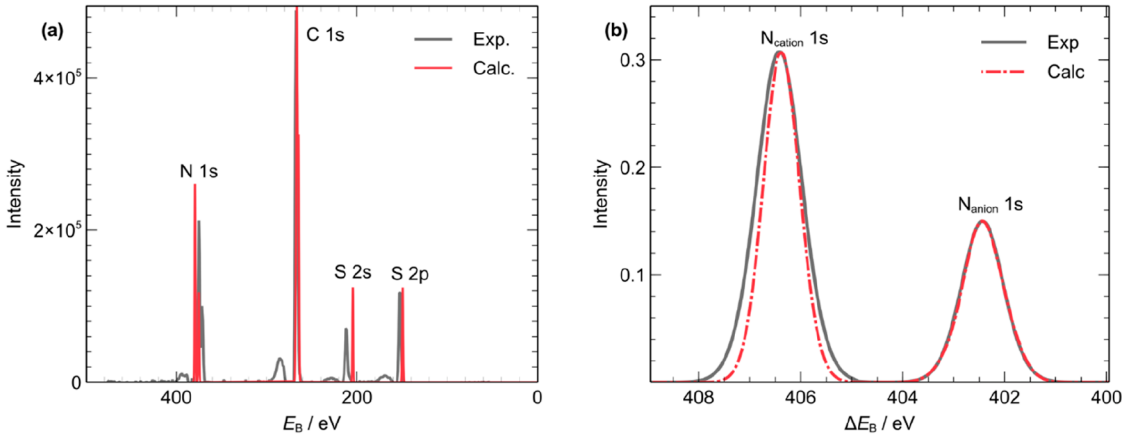

Figure 3. Initial-state effect calculations. (a) Experimental survey scan (gray) overlaid with the calculated survey scan (red). Calculated scan was shifted by +21.2 eV, and intensities were corrected using the C 1s peak. The calculated peaks were broadened with a width of 1 eV to mimic experimental broadening. (b) High-resolution scan of N 1s peaks. The calculated peaks were broadened with a 0.7 eV width to mimic experimental broadening.

https://doi.org/10.1021/acs.jpcb.2c06372
J. Phys. Chem. B 2022, 126, 10500−10509

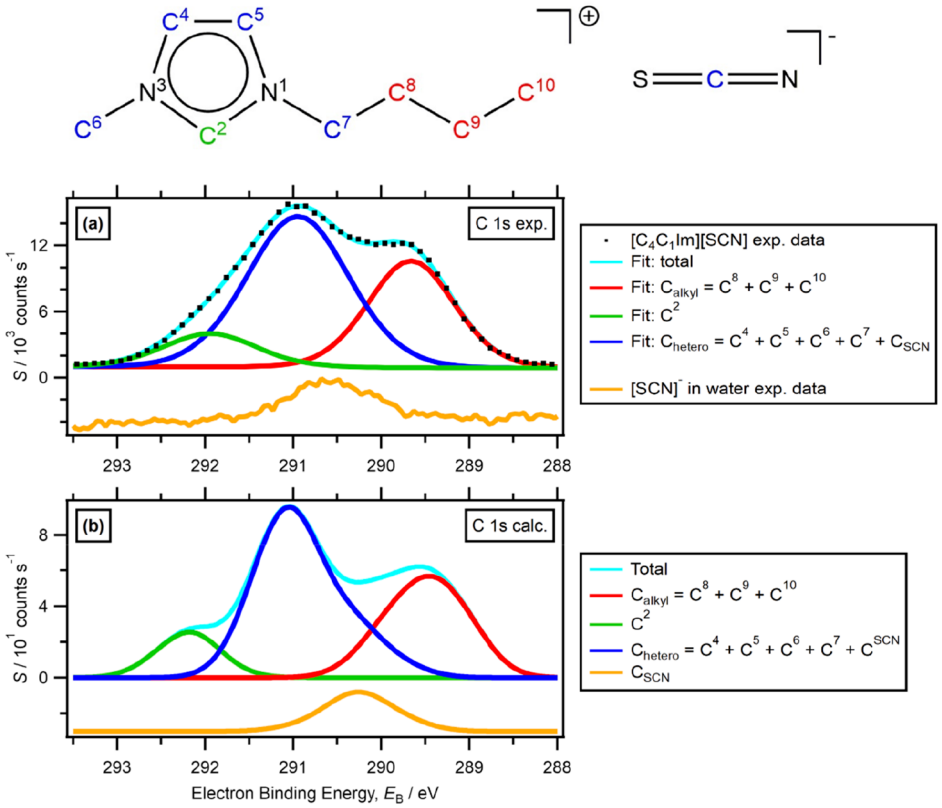

Figure 4. C 1s XPS. (a) Experimental C 1s peak fitting model for $[C_4C_1Im][SCN]$ published in ref 93; fitted with peaks for C_{alkyl}, C_{hetero}, and C^2. C_{hetero} is likely to contain contributions from the C_{anion} peak, increasing its FWHM. Experimental peak of C_{SCN} from K[SCN] in water. (b) Peaks calculated in this work, with a width function of 1 eV (see Section 2.5 for more details), separated into C_{alkyl}, C_{hetero}, C^2, and C_{anion}. Calculated C_{SCN} extracted for comparison to experimental E_B. Charge referencing for XP spectra is explained in Section 2.1.

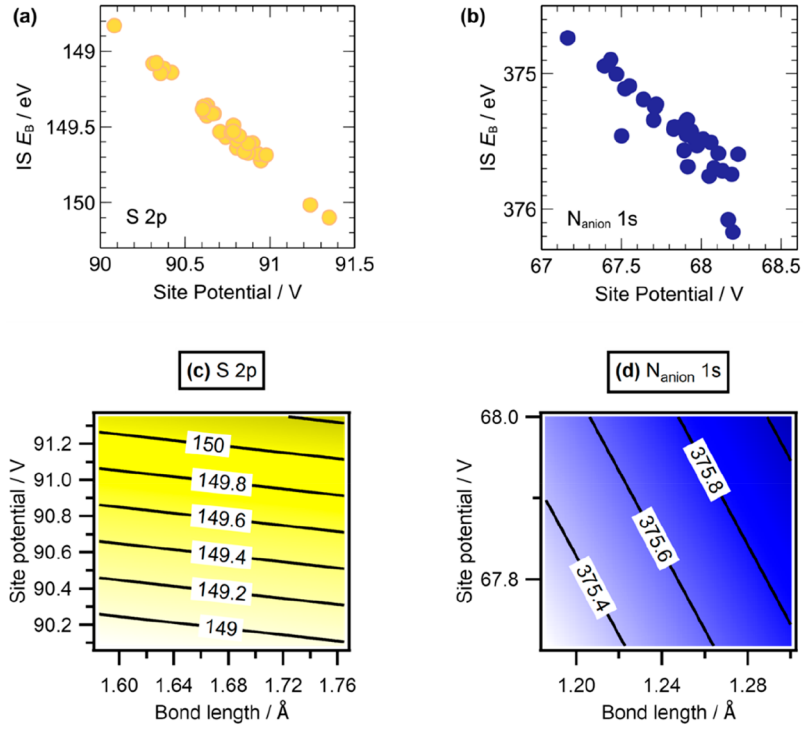

Figure 5. Correlation of IS E_B with site potential for (a) S 2p (yellow) and (b) N_{anion} 1s (blue). Contour maps of bilinear prediction models for (c) S 2p (yellow) and (d) N_{anion} 1s (blue) with E_B being a function of both the site potential and the bond length.

https://doi.org/10.1021/acs.jpcb.2c06372
J. Phys. Chem. B 2022, 126, 10500−10509

comparison with calculated peaks (Figure 4b) of the same species shows very good agreement—each peak position is matched within 0.1 eV. The experimental FWHM of C bonded to a single N (blue, C_{hetero}) is larger than the calculated, due to the unresolved $[SCN]^-$ contribution in the experimental fitting.

3.2. Peak Broadening. In the DFT calculations, instrumental and lifetime broadening are not simulated. A comparison between measured and calculated data of N_{anion} 1s and N_{cation} 1s peaks shows a very good N_{anion} 1s broadening match and a good N_{cation} 1s match (Figure 3b). A visual assessment of the same plot, but with a 0.5 eV width function, shows that the peaks do not match as well, and some asymmetry is present (ESI Figure S1). Experimental broadening for this data set is estimated as apparatus contributions of ∼0.45 to 0.65 eV and lifetime contributions of 0.054 and 0.115 eV for S 2p and N 1s, respectively, totaling ∼0.5 eV;[110,111] charging contributions are negligible.[109] Using an apparatus broadening value of 0.65 eV, the calculated structural broadening values were found to be in the range of 0.55 to 0.82 eV.

Testing increased sample sizes did not increase the N_{cation} 1s peak width to provide a better match to the experimental width, and only a slight improvement in peak symmetry was noted. There are two possible explanations for the slight peak width discrepancy in the spectrum: (i) the AIMD calculation is lacking accuracy in the disorder description of the system, or (ii) the experimental broadening value is underestimated. As the experimental broadening value is not an exact estimate and is likely to fluctuate between calibration and successive experiments, we believe the latter is the most likely source of the slight discrepancy.

3.3. Effects of Intraion and Interion Interactions on the Core-Level Binding Energies. Intraion interactions were analyzed through comparison of S−C bond length to the relevant $E_B(S_{anion}\ 2p)$ and N−C bond length to $E_B(N_{anion}\ 1s)$. Both plots produced a weak linear correlation (ESI Figure S2). Visual assessment and the RDFs for the analysis of short-range interactions did not produce a clear pattern of short-range interactions in relation to E_B, and this was not investigated further. Neither short-range nor intraion effects were found to be the dominant influence over E_B fluctuations. Longer-range interactions were characterized by calculating the site potential at each atom. The site potential is defined in VASP as the average of the electrostatic potential in the core region of a given atom. This site potential is affected by both short-range and long-range interactions. Plots of site potentials against E_B for each atom clearly demonstrated that $E_B(S_{anion}\ 2p)$ correlates almost perfectly with site potential, with very little deviation (Figure 5a). Although $E_B(N_{anion}\ 1s)$ also correlates very well with site potential, the deviation is slightly higher than for S 2p (Figure 5b). We successfully interpreted these patterns by further comparison with internal bond lengths in the form of a multiple regression model for E_B, based on both site potential and bond length values. The multiple regression produced a new model for E_B prediction (Figure 5c,d) which was compared against the actual calculated E_B. The model was found to be highly accurate, with a root-mean-square deviation (RMSD) of only 0.01 and 0.02 eV for S_{anion} 2p and N_{anion} 1s, respectively. In comparison to the linear regressions, which have RMSD values of 0.03 and 0.10 eV, respectively, accuracy is increased substantially, particularly for N_{anion} 1s.

The strong correlation of $E_B(S\ 2p)$ with site potential was assumed to be the result of the large, highly polarizable nature of the atom.[112] The electron cloud is understood to be more susceptible to the influence of collective electrons in a disordered bulk IL system than an atom like nitrogen, which is smaller and denser than sulfur. The valence and core electrons of a nitrogen atom were expected to be influenced more strongly by the N−C internal bond length than the sulfur atom is by the S−C internal bond length, due to the higher electron density in the N−C bond. Calculations found that when the S−C or N−C bond was altered in turn, the $E_B(N_{anion}$ 1s) undergoes higher energy changes with the same % bond length variation (Figure 6).

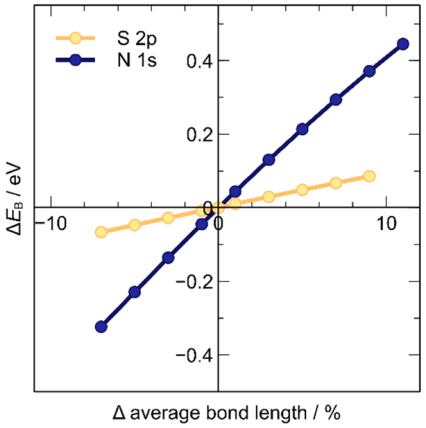

Figure 6. Plot of E_B change with variation of internal bond length in the anion $[SCN]^-$. Bond S−C for S_{anion} 2p and N−C for N_{anion} 1s.

The finding that E_B correlates very well with site potential shows that single ion pair studies are insufficient to describe the structure and interactions within a real IL system. Single ion or ion pair calculations are, by definition, based on the assumption that short-range intramolecular interactions dominate E_B broadening. Gas-phase models seem to overestimate the cation−anion interaction when the long-range structure is missing.[113] A slight improvement to this is an implicit solvent model or ionic pair "clusters"; however, these models cannot explicitly simulate long-range disorder of the liquid system. Focusing on a single ion pair increases chances of error when calculating E_B. This study found an ∼1 eV range in E_B fluctuations for a single atom type (Figure 2). A single ion pair, especially when optimized, could fall within the extremes of this range, rather than in the middle, or average of this range of E_B. Particularly when resolving shifts of <0.5 eV, this value has been shown to be within our error margin, and any findings related to a shift of this size may be entirely insignificant. This would likely result in inaccurate conclusions on the bulk system.

4. CONCLUSIONS

This study found a strong correlation between experiment and DFT calculations, demonstrating for the first time that IS contributions were the primary contributor to E_B values in the IL $[C_4C_1Im][SCN]$. This system is representative of a wide array of ILs, suggesting that IS effects would be the primary contributor to most ILs. Our finding suggests that either FS effects are negligible or are similar across all atoms, so do not contribute to peak separations. Furthermore, we confirm that

https://doi.org/10.1021/acs.jpcb.2c06372
J. Phys. Chem. B 2022, 126, 10500−10509

the effect of the anion on the cation, observed using XPS for many ILs, was driven by an IS effect. We confirmed that E_B was closely linked to site potential in the anion of $[C_4C_1Im][SCN]$. The site potential is influenced by all (both short- and long-range) interactions of the bulk system. We found no evidence to show that short-range, intermolecular interactions are sufficient on their own to describe the liquid phase E_B variation. Site potential did not offer a perfect correlation with E_B. The discrepancy was found to mostly correspond to intramolecular bond length fluctuations. With both site potentials and internal bond lengths, we produced a predictive model for E_B, which was found to be highly accurate for this IL.

■ ASSOCIATED CONTENT

Supporting Information

The Supporting Information is available free of charge at https://pubs.acs.org/doi/10.1021/acs.jpcb.2c06372.

Plot of high-resolution N 1s scan with 0.5 eV broadening; plots of IS E_B vs internal bond length for S 2p and N 1s (PDF)

■ AUTHOR INFORMATION

Corresponding Author

Kevin R. J. Lovelock − *Department of Chemistry, University of Reading, Reading RG6 6DX, U.K.;* orcid.org/0000-0003-1431-269X; Email: k.r.j.lovelock@reading.ac.uk

Authors

Ekaterina Gousseva − *Department of Chemistry, University of Reading, Reading RG6 6DX, U.K.*

Scott D. Midgley − *Department of Chemistry, University of Reading, Reading RG6 6DX, U.K.*

Jake M. Seymour − *Department of Chemistry, University of Reading, Reading RG6 6DX, U.K.*

Robert Seidel − *Helmholtz-Zentrum Berlin für Materialien und Energie (HZB), Berlin 14109, Germany;* orcid.org/0000-0003-2613-4106

Ricardo Grau-Crespo − *Department of Chemistry, University of Reading, Reading RG6 6DX, U.K.;* orcid.org/0000-0001-8845-1719

Complete contact information is available at: https://pubs.acs.org/10.1021/acs.jpcb.2c06372

Author Contributions

K.R.J.L. and R.G.C. conceptualized the study and supervised the work. E.G. performed the computer simulations, with help from S.D.M. J.M.S., K.R.J.L., and R.S. contributed the experimental part. E.G. wrote the original manuscript draft. All authors contributed to the writing of the manuscript.

Notes

The authors declare no competing financial interest.

■ ACKNOWLEDGMENTS

We are grateful to the UK Materials and Molecular Modeling Hub for access to the Young supercomputer facility, which is partially funded by the EPSRC (EP/T022213/1). This work also used the ARCHER2 UK National Supercomputing Service, via the Materials Chemistry Consortium, which is also funded by EPRSC (EP/R029431/1). K.R.J.L. acknowledges support from a Royal Society University Research Fellowship (URF\R\150353). J.M.S. acknowledges support from a Royal Society University Research Fellowship Enhancement Award (RGF\EA\180089). E.G. acknowledges support from a Royal Society Research Grant for Research Fellows (RGF\R1\180053). R.S. acknowledges funding from the German Research Foundation (DFG) through an Emmy-Noether grant (SE 2253/3-1). We thank the Helmholtz-Zentrum Berlin für Materialien und Energie for the allocation of synchrotron radiation beamtime (proposal 202-09664).

■ REFERENCES

(1) Lovelock, K. R. J.; Villar-Garcia, I. J.; Maier, F.; Steinrück, H. P.; Licence, P. Photoelectron spectroscopy of ionic liquid-based interfaces. *Chem. Rev.* **2010**, *110* (9), 5158−90.

(2) Welton, T. Ionic liquids in catalysis. *Coord. Chem. Rev.* **2004**, *248* (21−24), 2459−2477.

(3) Plechkova, N. V.; Seddon, K. R. Applications of ionic liquids in the chemical industry. *Chem. Soc. Rev.* **2008**, *37* (1), 123−50.

(4) Chiappe, C.; Pieraccini, D. Ionic liquids: solvent properties and organic reactivity. *J. Phys. Org. Chem.* **2005**, *18* (4), 275−297.

(5) Khan, A. S.; Man, Z.; Arvina, A.; Bustam, M. A.; Nasrullah, A.; Ullah, Z.; Sarwono, A.; Muhammad, N. Dicationic imidazolium based ionic liquids: Synthesis and properties. *J. Mol. Liq.* **2017**, *227*, 98−105.

(6) Hallett, J. P.; Welton, T. Room-Temperature Ionic Liquids: Solvents for Synthesis and Catalysis. 2. *Chem. Rev.* **2011**, *111* (5), 3508−3576.

(7) Wasserscheid, P.; Welton, T.*Ionic Liquids in Synthesis*; Wiley-VCH: Weinheim, 2008.

(8) Wilkes, J. Properties of ionic liquid solvents for catalysis. *J. Mol. Catal. A: Chem.* **2004**, *214* (1), 11−17.

(9) Philippi, F.; Pugh, D.; Rauber, D.; Welton, T.; Hunt, P. A. Conformational design concepts for anions in ionic liquids. *Chemical Science* **2020**, *11* (25), 6405−6422.

(10) Koutsoukos, S.; Philippi, F.; Malaret, F.; Welton, T. A review on machine learning algorithms for the ionic liquid chemical space. *Chem. Sci.* **2021**, *12* (20), 6820−6843.

(11) Holloczki, O.; Malberg, F.; Welton, T.; Kirchner, B. On the origin of ionicity in ionic liquids. Ion pairing versus charge transfer. *Phys. Chem. Chem. Phys.* **2014**, *16* (32), 16880−90.

(12) Philippi, F.; Goloviznina, K.; Gong, Z.; Gehrke, S.; Kirchner, B.; Padua, A. A. H.; Hunt, P. A. Charge transfer and polarisability in ionic liquids: a case study. *Phys. Chem. Chem. Phys.* **2022**, *24* (5), 3144−3162.

(13) Macchieraldo, R.; Esser, L.; Elfgen, R.; Voepel, P.; Zahn, S.; Smarsly, B. M.; Kirchner, B. Hydrophilic Ionic Liquid Mixtures of Weakly and Strongly Coordinating Anions with and without Water. *ACS Omega* **2018**, *3* (8), 8567−8582.

(14) Bedrov, D.; Piquemal, J. P.; Borodin, O.; MacKerell, A. D., Jr.; Roux, B.; Schroder, C. Molecular Dynamics Simulations of Ionic Liquids and Electrolytes Using Polarizable Force Fields. *Chem. Rev.* **2019**, *119* (13), 7940−7995.

(15) Briggs, D.; Grant, J. T.*Surface Analysis by Auger and X-Ray Photoelectron Spectroscopy*; IM Publications: Manchester, 2003.

(16) Vickerman, J. C.; Gilmore, I. S.*Surface Analysis: The Principal Techniques*; John Wiley & Sons: Chichester, 2009.

(17) Lovelock, K. R. J.; Licence, P.Ionic Liquids Studied at Ultra-High Vacuum. In *Ionic Liquids UnCOILed: Critical Expert Overviews*; Seddon, K. R., Plechkova, N. V., Eds.; Wiley: Oxford, 2012; pp 251−282.

(18) Smith, E. F.; Rutten, F. J.; Villar-Garcia, I. J.; Briggs, D.; Licence, P. Ionic liquids in vacuo: analysis of liquid surfaces using ultra-high-vacuum techniques. *Langmuir* **2006**, *22* (22), 9386−92.

(19) Steinrück, H. P. Recent developments in the study of ionic liquid interfaces using X-ray photoelectron spectroscopy and potential future directions. *Phys. Chem. Chem. Phys.* **2012**, *14* (15), 5010−29.

(20) Steinrück, H. P.; Libuda, J.; Wasserscheid, P.; Cremer, T.; Kolbeck, C.; Laurin, M.; Maier, F.; Sobota, M.; Schulz, P. S.; Stark, M. Surface science and model catalysis with ionic liquid-modified materials. *Adv. Mater.* **2011**, *23* (22−23), 2571−87.

(21) Maier, F.; Cremer, T.; Kolbeck, C.; Lovelock, K. R. J.; Paape, N.; Schulz, P. S.; Wasserscheid, P.; Steinrück, H. P. Insights into the surface composition and enrichment effects of ionic liquids and ionic liquid mixtures. *Phys. Chem. Chem. Phys.* **2010**, *12* (8), 1905−15.
(22) Steinrück, H.-P.; Wasserscheid, P. Ionic Liquids in Catalysis. *Catal. Lett.* **2015**, *145* (1), 380−397.
(23) Hohlneicher, G.; Pulm, H.; Freund, H. J. On the Separation of Initial and Final-State Effects in Photoelectron-Spectroscopy Using an Extension of the Auger-Parameter Concept. *J. Electron Spectrosc* **1985**, *37* (3), 209−224.
(24) Egelhoff, W. F. Core-level binding-energy shifts at surfaces and in solids. *Surf. Sci. Rep.* **1987**, *6* (6−8), 253−415.
(25) Cremer, T.; Kolbeck, C.; Lovelock, K. R. J.; Paape, N.; Wölfel, R.; Schulz, P. S.; Wasserscheid, P.; Weber, H.; Thar, J.; Kirchner, B.; et al. Towards a molecular understanding of cation-anion interactions-probing the electronic structure of imidazolium ionic liquids by NMR spectroscopy, X-ray photoelectron spectroscopy and theoretical calculations. *Chemistry* **2010**, *16* (30), 9018−33.
(26) Men, S.; Lovelock, K. R. J.; Licence, P. X-ray photoelectron spectroscopy of pyrrolidinium-based ionic liquids: cation-anion interactions and a comparison to imidazolium-based analogues. *Phys. Chem. Chem. Phys.* **2011**, *13* (33), 15244−55.
(27) Hurisso, B. B.; Lovelock, K. R. J.; Licence, P. Amino acid-based ionic liquids: using XPS to probe the electronic environment via binding energies. *Phys. Chem. Chem. Phys.* **2011**, *13* (39), 17737−48.
(28) Taylor, A. W.; Men, S.; Clarke, C. J.; Licence, P. Acidity and basicity of halometallate-based ionic liquids from X-ray photoelectron spectroscopy. *RSC Adv.* **2013**, *3* (24), 9436−9445.
(29) Villar-Garcia, I. J.; Lovelock, K. R. J.; Men, S.; Licence, P. Tuning the electronic environment of cations and anions using ionic liquid mixtures. *Chem. Sci.* **2014**, *5* (6), 2573−2579.
(30) Blundell, R. K.; Licence, P. Quaternary ammonium and phosphonium based ionic liquids: a comparison of common anions. *Phys. Chem. Chem. Phys.* **2014**, *16* (29), 15278−88.
(31) Blundell, R. K.; Licence, P. Tuning cation-anion interactions in ionic liquids by changing the conformational flexibility of the cation. *Chem. Commun. (Camb)* **2014**, *50* (81), 12080−3.
(32) Men, S.; Mitchell, D. S.; Lovelock, K. R. J.; Licence, P. X-ray Photoelectron Spectroscopy of Pyridinium-Based Ionic Liquids: Comparison to Imidazolium- and Pyrrolidinium-Based Analogues. *ChemPhysChem* **2015**, *16* (10), 2211−8.
(33) Longo, L. S.; Smith, E. F.; Licence, P. Study of the Stability of 1-Alkyl-3-methylimidazolium Hexafluoroantimonate(V) Based Ionic Liquids Using X-ray Photoelectron Spectroscopy. *ACS Sustainable Chem. Eng.* **2016**, *4* (11), 5953−5962.
(34) Men, S.; Lovelock, K. R. J.; Licence, P. X-ray photoelectron spectroscopy of trihalide ionic liquids: Comparison to halide-based analogues, anion basicity and beam damage. *Chem. Phys. Lett.* **2017**, *679*, 207−211.
(35) Men, S.; Licence, P.; Do-Thanh, C.-L.; Luo, H.; Dai, S. X-ray photoelectron spectroscopy of piperidinium ionic liquids: a comparison to the charge delocalised pyridinium analogues. *Phys. Chem. Chem. Phys.* **2020**, *22* (21), 11976−11983.
(36) Men, S.; Licence, P.; Luo, H.; Dai, S. Tuning the Cation-Anion Interactions by Methylation of the Pyridinium Cation: An X-ray Photoelectron Spectroscopy Study of Picolinium Ionic Liquids. *J. Phys. Chem. B* **2020**, *124* (30), 6657−6663.
(37) Santos, A. R.; Blundell, R. K.; Licence, P. XPS of guanidinium ionic liquids: a comparison of charge distribution in nitrogenous cations. *Phys. Chem. Chem. Phys.* **2015**, *17* (17), 11839−47.
(38) Santos, A. R.; Hanson-Heine, M. W. D.; Besley, N. A.; Licence, P. The impact of sulfur functionalisation on nitrogen-based ionic liquid cations. *Chem. Commun. (Camb)* **2018**, *54* (81), 11403−11406.
(39) Clarke, C. J.; Maxwell-Hogg, S.; Smith, E. F.; Hawker, R. R.; Harper, J. B.; Licence, P. Resolving X-ray photoelectron spectra of ionic liquids with difference spectroscopy. *Phys. Chem. Chem. Phys.* **2019**, *21* (1), 114−123.
(40) Dick, E. J.; Fouda, A. E. A.; Besley, N. A.; Licence, P. Probing the electronic structure of ether functionalised ionic liquids using X-ray photoelectron spectroscopy. *Phys. Chem. Chem. Phys.* **2020**, *22* (3), 1624−1631.
(41) Apperley, D. C.; Hardacre, C.; Licence, P.; Murphy, R. W.; Plechkova, N. V.; Seddon, K. R.; Srinivasan, G.; Swadzba-Kwasny, M.; Villar-Garcia, I. J. Speciation of chloroindate(III) ionic liquids. *Dalton Trans* **2010**, *39* (37), 8679−87.
(42) Taylor, A. W.; Qiu, F.; Villar-Garcia, I. J.; Licence, P. Spectroelectrochemistry at ultrahigh vacuum: in situ monitoring of electrochemically generated species by X-ray photoelectron spectroscopy. *Chem. Commun. (Camb)* **2009**, No. 39, 5817−9.
(43) Men, S.; Lovelock, K. R. J.; Licence, P. Directly probing the effect of the solvent on a catalyst electronic environment using X-ray photoelectron spectroscopy. *RSC Adv.* **2015**, *5* (45), 35958−35965.
(44) Men, S.; Jiang, J. X-ray photoelectron spectroscopy as a probe of the interaction between rhodium acetate and ionic liquids. *Chem. Phys. Lett.* **2016**, *646*, 125−129.
(45) Men, S.; Lovelock, K. R. J.; Licence, P. X-ray photoelectron spectroscopy as a probe of rhodium-ligand interaction in ionic liquids. *Chem. Phys. Lett.* **2016**, *645*, 53−58.
(46) Men, S.; Jiang, J. Probing the impact of the cation acidity on the cation-anion interaction in ionic liquids by X-ray photoelectron spectroscopy. *Chem. Phys. Lett.* **2017**, *677*, 60−64.
(47) Men, S.; Jiang, J.; Licence, P. Spectroscopic analysis of 1-butyl-2,3-dimethylimidazolium ionic liquids: Cation-anion interactions. *Chem. Phys. Lett.* **2017**, *674*, 86−89.
(48) Men, S.; Jiang, J.; Liu, Y. X-Ray Photoelectron Spectroscopy of Imidazolium Zwitterionic Salts: Comparison to Acetate Analogs and the Impact of the Alkyl Chain Length on the Charge Distribution. *J. Appl. Spectrosc.* **2017**, *84* (5), 906−910.
(49) Men, S.; Licence, P. Tuning the electronic environment of the anion by using binary ionic liquid mixtures. *Chem. Phys. Lett.* **2017**, *681*, 40−43.
(50) Men, S.; Licence, P. Probing the electronic environment of binary and ternary ionic liquid mixtures by X-ray photoelectron spectroscopy. *Chem. Phys. Lett.* **2017**, *686*, 74−77.
(51) Liu, Y.; Ma, C.; Men, S.; Jin, Y. An investigation of trioctylmethylammonium ionic liquids by X-ray photoelectron spectroscopy: The cation-anion interaction. *J. Electron Spectrosc* **2018**, *223*, 79−83.
(52) Men, S.; Jiang, J. Probing the Formation of the NHC-Palladium Species in Ionic Liquids by X-ray Photoelectron Spectroscopy. *Russian Journal of Physical Chemistry A* **2018**, *92* (8), 1627−1630.
(53) Men, S.; Jiang, J. X-Ray Photoelectron Spectroscopy of Chlorometallate Ionic Liquids: Speciation and Anion Basicity. *J. Appl. Spectrosc.* **2018**, *85* (1), 55−60.
(54) Men, S.; Jin, Y. X-ray Photoelectron Spectroscopy of Imidazolium-Based Zwitterions: The Intramolecular Charge-Transfer Effect. *Russian Journal of Physical Chemistry A* **2018**, *92* (11), 2337−2340.
(55) Men, S.; Rong, J.; Zhang, T.; Wang, X.; Feng, L.; Liu, C.; Jin, Y. Spectroscopic Analysis of 1-Butyl-3-methylimidazolium Ionic Liquids: Selection of the Charge Reference and the Electronic Environment. *Russian Journal of Physical Chemistry A* **2018**, *92* (10), 1975−1979.
(56) Liu, Y.; Chen, X.; Men, S.; Licence, P.; Xi, F.; Ren, Z.; Zhu, W. The impact of cation acidity and alkyl substituents on the cation-anion interactions of 1-alkyl-2,3-dimethylimidazolium ionic liquids. *Phys. Chem. Chem. Phys.* **2019**, *21* (21), 11058−11065.
(57) Wei, L.; Men, S. X-ray Photoelectron Spectroscopy of 1-Butyl-2,3-Dimethylimidazolium Ionic Liquids: Charge Correction Methods and Electronic Environment of the Anion. *Russian Journal of Physical Chemistry A* **2019**, *93* (13), 2676−2680.
(58) He, Y.; Men, S. Charge Distribution of Phosphonium Ionic Liquids: Phosphonium versus Phosphate. *Russian Journal of Physical Chemistry A* **2020**, *94* (10), 2091−2095.
(59) Men, S.; Jin, Y.; Licence, P. Probing the impact of the N3-substituted alkyl chain on the electronic environment of the cation and the anion for 1,3-dialkylimidazolium ionic liquids. *Phys. Chem. Chem. Phys.* **2020**, *22* (30), 17394−17400.

https://doi.org/10.1021/acs.jpcb.2c06372
J. Phys. Chem. B 2022, 126, 10500−10509

(60) Mu, R.; Deng, A.; Men, S. Tribromide Ionic Liquids: Probing the Charge Distribution of the Anion by XPS. *Russian Journal of Physical Chemistry A* **2020**, *94* (5), 1053−1056.
(61) Wei, L.; Wang, S.; Men, S. Electronic Effects in the Structure of 1-Ethyl-3-Methylimidazolium Ionic Liquids. *Russian Journal of Physical Chemistry A* **2021**, *95* (4), 736−740.
(62) Lovelock, K. R. J.; Kolbeck, C.; Cremer, T.; Paape, N.; Schulz, P. S.; Wasserscheid, P.; Maier, F.; Steinrück, H. P. Influence of different substituents on the surface composition of ionic liquids studied using ARXPS. *J. Phys. Chem. B* **2009**, *113* (9), 2854−64.
(63) Taccardi, N.; Niedermaier, I.; Maier, F.; Steinrück, H. P.; Wasserscheid, P. Cyclic thiouronium ionic liquids: physicochemical properties and their electronic structure probed by X-ray induced photoelectron spectroscopy. *Chemistry* **2012**, *18* (27), 8288−91.
(64) Heller, B. S. J.; Kolbeck, C.; Niedermaier, I.; Dommer, S.; Schatz, J.; Hunt, P.; Maier, F.; Steinrück, H. P. Surface Enrichment in Equimolar Mixtures of Non-Functionalized and Functionalized Imidazolium-Based Ionic Liquids. *ChemPhysChem* **2018**, *19* (14), 1733−1745.
(65) Reinmöller, M.; Ulbrich, A.; Ikari, T.; Preiss, J.; Höfft, O.; Endres, F.; Krischok, S.; Beenken, W. J. Theoretical reconstruction and elementwise analysis of photoelectron spectra for imidazolium-based ionic liquids. *Phys. Chem. Chem. Phys.* **2011**, *13* (43), 19526−33.
(66) Fogarty, R. M.; Rowe, R.; Matthews, R. P.; Clough, M. T.; Ashworth, C. R.; Brandt, A.; Corbett, P. J.; Palgrave, R. G.; Smith, E. F.; Bourne, R. A.; et al. Atomic charges of sulfur in ionic liquids: experiments and calculations. *Faraday Discuss.* **2018**, *206*, 183−201.
(67) Fogarty, R. M.; Matthews, R. P.; Ashworth, C. R.; Brandt-Talbot, A.; Palgrave, R. G.; Bourne, R. A.; Vander Hoogerstraete, T.; Hunt, P. A.; Lovelock, K. R. J. Experimental validation of calculated atomic charges in ionic liquids. *J. Chem. Phys.* **2018**, *148* (19), 193817.
(68) Lembinen, M.; Nõmmiste, E.; Ers, H.; Docampo-Álvarez, B.; Kruusma, J.; Lust, E.; Ivaništšev, V. B. Calculation of core-level electron spectra of ionic liquids. *Int. J. Quantum Chem.* **2020**, *120* (14), No. e26247.
(69) Rangan, S.; Viereck, J.; Bartynski, R. A. Electronic Properties of Cyano Ionic Liquids: a Valence Band Photoemission Study. *J. Phys. Chem. B* **2020**, *124* (36), 7909−7917.
(70) Dhungana, K. B.; Faria, L. F.; Wu, B.; Liang, M.; Ribeiro, M. C.; Margulis, C. J.; Castner, E. W., Jr. Structure of cyano-anion ionic liquids: X-ray scattering and simulations. *J. Chem. Phys.* **2016**, *145* (2), 024503.
(71) Liu, J.; Zhang, H.; Li, Y.; Liu, Z. Disorder in Aqueous Solutions and Peak Broadening in X-ray Photoelectron Spectroscopy. *J. Phys. Chem. B* **2018**, *122* (46), 10600−10606.
(72) Sprenger, D.; Anderson, O. Deconvolution of XPS spectra. *Fresenius' Journal of Analytical Chemistry* **1991**, *341* (1−2), 116−120.
(73) Baer, D. R.; Artyushkova, K.; Cohen, H.; Easton, C. D.; Engelhard, M.; Gengenbach, T. R.; Greczynski, G.; Mack, P.; Morgan, D. J.; Roberts, A. XPS guide: Charge neutralization and binding energy referencing for insulating samples. *Journal of Vacuum Science & Technology A* **2020**, *38* (3), 031204.
(74) Fuggle, J. C.; Alvarado, S. F. Core-level lifetimes as determined by x-ray photoelectron spectroscopy measurements. *Phys. Rev. A* **1980**, *22* (4), 1615−1624.
(75) Lundholm, M.; Siegbahn, H.; Holmberg, S.; Arbman, M. Core electron spectroscopy of water solutions. *J. Electron Spectrosc* **1986**, *40* (2), 163−180.
(76) Winter, B.; Aziz, E. F.; Hergenhahn, U.; Faubel, M.; Hertel, I. V. Hydrogen bonds in liquid water studied by photoelectron spectroscopy. *J. Chem. Phys.* **2007**, *126* (12), 124504.
(77) Kirchner, B.; di Dio, P. J.; Hutter, J. Real-world predictions from ab initio molecular dynamics simulations. *Top Curr. Chem.* **2011**, *307*, 109−53.
(78) Pensado, A. S.; Brehm, M.; Thar, J.; Seitsonen, A. P.; Kirchner, B. Effect of dispersion on the structure and dynamics of the ionic liquid 1-ethyl-3-methylimidazolium thiocyanate. *ChemPhysChem* **2012**, *13* (7), 1845−53.
(79) Campetella, M.; Macchiagodena, M.; Gontrani, L.; Kirchner, B. Effect of alkyl chain length in protic ionic liquids: an AIMD perspective. *Mol. Phys.* **2017**, *115* (13), 1582−1589.
(80) Kiefer, J.; Noack, K.; Penna, T. C.; Ribeiro, M. C. C.; Weber, H.; Kirchner, B. Vibrational signatures of anionic cyano groups in imidazolium ionic liquids. *Vib. Spectrosc.* **2017**, *91*, 141−146.
(81) Cassone, G.; Sponer, J.; Saija, F. Ab Initio Molecular Dynamics Studies of the Electric-Field-Induced Catalytic Effects on Liquids. *Top. Catal.* **2022**, *65*, 40.
(82) Shah, J. K.Ab Initio Molecular Dynamics Simulations of Ionic Liquids. In *Annual Reports in Computational Chemistry*; Elsevier Science BV: Amsterdam, 2018; Vol. *14*, pp 95−122.
(83) Brehm, M.; Weber, H.; Pensado, A. S.; Stark, A.; Kirchner, B. Liquid Structure and Cluster Formation in Ionic Liquid/Water Mixtures - An Extensive ab initio Molecular Dynamics Study on 1-Ethyl-3-Methylimidazolium Acetate/Water Mixtures - Part. *Zeitschrift für Physikalische Chemie* **2013**, *227* (2−3), 177−204.
(84) Brussel, M.; Brehm, M.; Voigt, T.; Kirchner, B. Ab initio molecular dynamics simulations of a binary system of ionic liquids. *Phys. Chem. Chem. Phys.* **2011**, *13* (30), 13617−20.
(85) Del Popolo, M. G.; Lynden-Bell, R. M.; Kohanoff, J. Ab initio molecular dynamics simulation of a room temperature ionic liquid. *J. Phys. Chem. B* **2005**, *109* (12), 5895−902.
(86) Payal, R. S.; Balasubramanian, S. Dissolution of cellulose in ionic liquids: an ab initio molecular dynamics simulation study. *Phys. Chem. Chem. Phys.* **2014**, *16* (33), 17458−65.
(87) Zahn, S.; Brehm, M.; Brüssel, M.; Hollóczki, O.; Kohagen, M.; Lehmann, S.; Malberg, F.; Pensado, A. S.; Schöppke, M.; Weber, H.; Kirchner, B. Understanding ionic liquids from theoretical methods. *J. Mol. Liq.* **2014**, *192*, 71−76.
(88) Ghatee, M. H.; Ansari, Y. Ab initio molecular dynamics simulation of ionic liquids. *J. Chem. Phys.* **2007**, *126* (15), 154502.
(89) Bhargava, B. L.; Yasaka, Y.; Klein, M. L. Hydrogen evolution from formic acid in an ionic liquid solvent: a mechanistic study by ab initio molecular dynamics. *J. Phys. Chem. B* **2011**, *115* (48), 14136−40.
(90) Goel, H.; Windom, Z. W.; Jackson, A. A.; Rai, N. CO_2 sorption in triethyl(butyl)phosphonium 2-cyanopyrrolide ionic liquid via first principles simulations. *J. Mol. Liq.* **2019**, *292*, 111323.
(91) Clarke-Hannaford, J.; Breedon, M.; Rüther, T.; Spencer, M. J. S. Stability of Boronium Cation-Based Ionic Liquid Electrolytes on the Li Metal Anode Surface. *ACS Appl. Energy Mater.* **2020**, *3* (6), 5497−5509.
(92) Esser, L.; Macchieraldo, R.; Elfgen, R.; Sieland, M.; Smarsly, B. M.; Kirchner, B. TiCl4 Dissolved in Ionic Liquid Mixtures from ab Initio Molecular Dynamics Simulations. *Molecules* **2021**, *26* (1), 79.
(93) Almeida, H. F. D.; Canongia Lopes, J. N.; Rebelo, L. P. N.; Coutinho, J. A. P.; Freire, M. G.; Marrucho, I. M. Densities and Viscosities of Mixtures of Two Ionic Liquids Containing a Common Cation. *Journal of Chemical & Engineering Data* **2016**, *61* (8), 2828−2843.
(94) Seddon, K. R.; Stark, A.; Torres, M.-J.Viscosity and Density of 1-Alkyl-3-methylimidazolium Ionic Liquids. In *Clean Solvents - Alternative Media for Chemical Reactions and Processing*; Abraham, M. A., Moens, L., Eds.; American Chemical Society: Washington, DC, 2002; pp 34−49.
(95) Seidel, R.; Pohl, M. N.; Ali, H.; Winter, B.; Aziz, E. F. Advances in liquid phase soft-x-ray photoemission spectroscopy: A new experimental setup at BESSY II. *Rev. Sci. Instrum.* **2017**, *88* (7), 073107.
(96) Seymour, J. M.; Gousseva, E.; Large, A. I.; Clarke, C. J.; Licence, P.; Fogarty, R. M.; Duncan, D. A.; Ferrer, P.; Venturini, F.; Bennett, R. A.; et al. Experimental measurement and prediction of ionic liquid ionisation energies. *Phys. Chem. Chem. Phys.* **2021**, *23* (37), 20957−20973.
(97) Haghani, A.; Hoffmann, M. M.; Iloukhani, H. Density, Speed of Sound, and Refractive Index of Binary Mixtures of 1-Butyl-3-

https://doi.org/10.1021/acs.jpcb.2c06372
J. Phys. Chem. B 2022, 126, 10500−10509

methylimidazolium Thiocyanate + 2-Alkanols (C3-C6) at Different Temperatures T = (288.15−338.15) K. *Journal of Chemical & Engineering Data* **2021**, *66* (5), 1956−1969.
(98) Perdew, J. P.; Burke, K.; Ernzerhof, M. Generalized Gradient Approximation Made Simple. *Phys. Rev. Lett.* **1996**, *77* (18), 3865−3868.
(99) Grimme, S. Accurate description of van der Waals complexes by density functional theory including empirical corrections. *J. Comput. Chem.* **2004**, *25* (12), 1463−73.
(100) Grimme, S. Semiempirical GGA-type density functional constructed with a long-range dispersion correction. *J. Comput. Chem.* **2006**, *27* (15), 1787−99.
(101) Kresse, G.; Furthmüller, J. Efficient iterative schemes for ab initio total-energy calculations using a plane-wave basis set. *Phys. Rev. B Condens Matter* **1996**, *54* (16), 11169−11186.
(102) Kresse, G.; Joubert, D. From ultrasoft pseudopotentials to the projector augmented-wave method. *Phys. Rev. B* **1999**, *59* (3), 1758−1775.
(103) Blöchl, P. E. Projector augmented-wave method. *Phys. Rev. B Condens Matter* **1994**, *50* (24), 17953−17979.
(104) Frisch, M. J.; Trucks, G. W.; Schlegel, H. B.; Scuseria, G. E.; Robb, M. A.; Cheeseman, J. R.; Scalmani, G.; Barone, V.; Petersson, G. A.; Nakatsuji, H.; et al.*Gaussian 16, Rev. C.01*; Gaussian, Inc.: Wallingford, CT, 2016.
(105) Petersson, G. A.; Al-Laham, M. A. A complete basis set model chemistry. II. Open-shell systems and the total energies of the first-row atoms. *J. Chem. Phys.* **1991**, *94* (9), 6081−6090.
(106) Petersson, G. A.; Bennett, A.; Tensfeldt, T. G.; Al-Laham, M. A.; Shirley, W. A.; Mantzaris, J. A complete basis set model chemistry. I. The total energies of closed-shell atoms and hydrides of the first-row elements. *J. Chem. Phys.* **1988**, *89* (4), 2193−2218.
(107) Becke, A. D. Density-functional thermochemistry. III. The role of exact exchange. *J. Chem. Phys.* **1993**, *98* (7), 5648−5652.
(108) Jain, V.; Biesinger, M. C.; Linford, M. R. The Gaussian-Lorentzian Sum, Product, and Convolution (Voigt) functions in the context of peak fitting X-ray photoelectron spectroscopy (XPS) narrow scans. *Appl. Surf. Sci.* **2018**, *447*, 548−553.
(109) Fogarty, R. M.; Palgrave, R. G.; Bourne, R. A.; Handrup, K.; Villar-Garcia, I. J.; Payne, D. J.; Hunt, P. A.; Lovelock, K. R. J. Electron spectroscopy of ionic liquids: experimental identification of atomic orbital contributions to valence electronic structure. *Phys. Chem. Chem. Phys.* **2019**, *21* (35), 18893−18910.
(110) Prince, K. C.; Vondráček, M.; Karvonen, J.; Coreno, M.; Camilloni, R.; Avaldi, L.; de Simone, M. A critical comparison of selected 1s and 2p core hole widths. *J. Electron Spectrosc* **1999**, *101*−*103*, 141−147.
(111) Pi, J. M.; Stella, M.; Fernando, N. K.; Lam, A. Y.; Regoutz, A.; Ratcliff, L. E. Predicting Core Level Photoelectron Spectra of Amino Acids Using Density Functional Theory. *J. Phys. Chem. Lett.* **2020**, *11* (6), 2256−2262.
(112) Heid, E.; Szabadi, A.; Schroder, C. Quantum mechanical determination of atomic polarizabilities of ionic liquids. *Phys. Chem. Chem. Phys.* **2018**, *20* (16), 10992−10996.
(113) Low, K.; Tan, S. Y. S.; Izgorodina, E. I. An ab initio Study of the Structure and Energetics of Hydrogen Bonding in Ionic Liquids. *Front Chem.* **2019**, *7*, 208.

https://doi.org/10.1021/acs.jpcb.2c06372
J. Phys. Chem. B 2022, 126, 10500−10509